Electronic supplementary information

Mechanochemical preparation of thermoplastic cellulose oleate by ball milling

De-Fa Hou, Meng-Lei Li, Cong Yan, Ling Zhou, Zheng-Ying Liu, Wei Yang and Ming-Bo Yang*

College of Polymer Science and Engineering, State Key Laboratory of Polymer Materials Engineering, Sichuan University, Chengdu 610065, P. R. China

**To whom correspondence should be addressed. Email: yangmb@scu.edu.cn*

Contents

1. Fabrication of amorphous regenerated cellulose cake (RCC)

Based on our previous researches[1, 2], RCC contained oleic acid that was fabricated by dissolution/regeneration and solvent exchange. To be specific, a transparent cellulose solution was first prepared by freezing-thawing MCC/sodium hydroxide (NaOH) aqueous suspension according to a well-established method with slight modifications[3]. In brief, NaOH (5 g) was dissolved into ultrapure water (95 ml), then dried MCC (2 g) was added and swelled for 3 h at room temperature. The steady suspension was cooled down to -18 °C to obtain a solid frozen mass, and the frozen solid was then allowed to thaw out at room temperature with drastically stirring to obtain a homogeneous cellulose solution. Then, cellulose solution (15.3 g) was instilled into ethanol (100 ml) with stirring to obtain regenerated cellulose (RC), then RC was neutralized by adding hydrochloric acid and washed several times by ethanol. Next, the ethanol in the products was exchanged for oleic acid by washing and vacuum-filtering, the step was repeated three times to acquire the amorphous RCC, and the weight of the obtained RCC was determined carefully before adding into stainless-steel jar. Besides, the oleic acid in the filtrate was recycled by rotary evaporation.

2. Preparation of regenerated cellulose aerogel (RCA)

To easily observe the morphology of RCC, the oleic acid in RCC was exchanged for *tert*-butanol by washing and vacuum-filtering for freeze-drying, and the fluffy RCA can be fabricated by further vacuum drying at 45 °C.

3. Mechanochemical synthesis of cellulose oleate (COE) from RCC

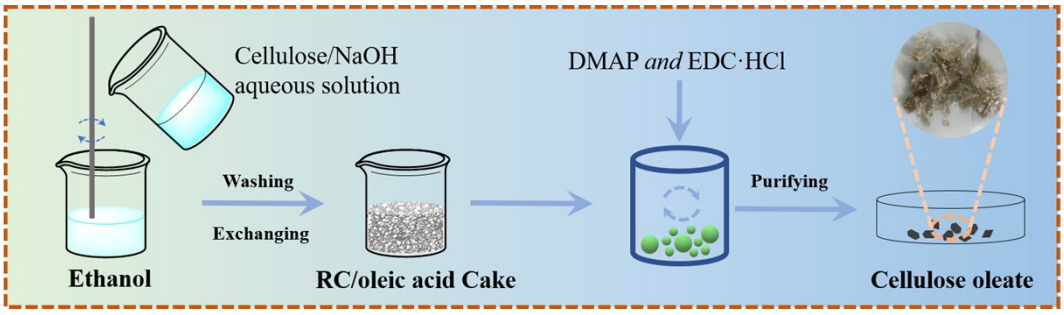

Fig. S1 Schematic presentation of mechanochemical synthesis of COE from RCC.

4. Esterification of cellulose with oleic acid in the presence of DMAP and EDC·HCl

The esterification of cellulose with a carboxylic acid in the presence of DMAP and EDC·HCl has been studied in many reports [4, 5]. In this reaction, EDC·HCl is a sacrificial activator of carboxylic acid involving the condensation of carboxylic acids into anhydrides. Subsequently, DMAP can convert the anhydride into a highly reactive species which reacts readily with cellulose to yield cellulose ester[4, 5].

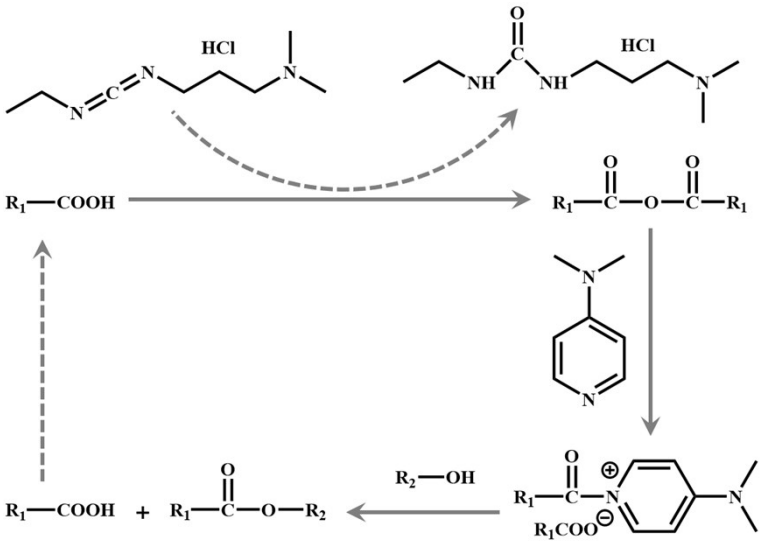

Scheme S1 The detailed synthetic scheme of the esterification between cellulose and carboxylic acid in the presence of DMAP and EDC·HCl.

5. Determining the degree of substitution (DS) of COE

DS values of all synthesized COEs were measured by using a well-established volumetric method[6, 7]. First, accurately weighted COE (*ca.* 0.2000 g) was saponified by KOH alcoholic solution (0.25 M, 40 ml) in an Erlenmeyer flask equipped with a reflux condenser at 70 °C for 17 h. After cooling, the resulting solution was titrated with a fresh hydrochloric acid solution (0.1 M) to release oleic acid. Finally, the DS values of COEs were calculated by the following equations (S1 and S2):

$$n = \frac{(V_0 - V_1)C_{HCl}}{1000} \qquad \text{Eq. (S1)}$$

$$DS = \frac{162n}{m - (M - 1)n} \qquad \text{Eq. (S2)}$$

Where V_0 and V_1 represented the volumes (unit: ml) of hydrochloric acid for the

neutralization of KOH alcoholic solution before and after the saponification of COE, respectively; C_{HCl} was the molar concentration (unit: mol l^{-1}) of the hydrochloric acid solution; m was the weight (unit: g) of COE. Besides, 162 denoted the molecular weight of AGU; and M denoted the molecular weight of an oleoyl group. The final DS value of each COE was an average of three measurements.

6. Chemical structures of OCEs synthesized under different reaction times

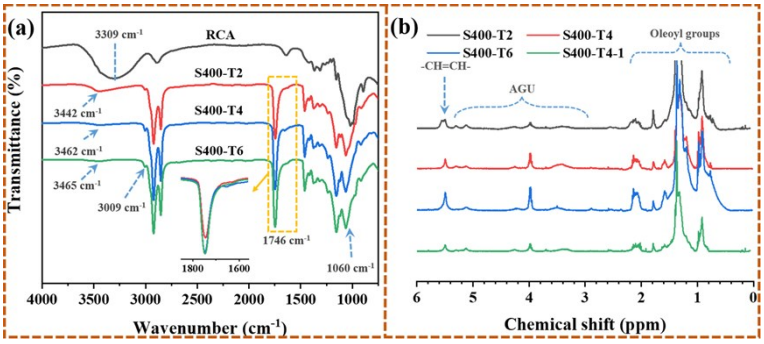

Fig. S2 ATR-IR spectra (a) and ^{1}H NMR spectra (b) of COEs synthesized under different reaction times (the rotational speed was fixed at 400 rpm), respectively.

7. Solubility of COEs in various organic solvents

Each COE (20 mg) was pulverized by grinding, and the powdery COE was dispersed in different organic solvents (10 ml) to investigate the solubility of COEs. As seen in Fig. S3, taking S400-T4 as an example, COE can be temporarily suspended in nonpolar solvents, indicated the nonpolar surface of the obtained COEs. Besides, S400-T4 can be well-dispersed in benzene after statically positing for 48 h. Based on the phenomena in Fig. S3, it can infer that COE can be slightly dissolved in benzene. Thus, benzene-d_6 was designated as the solvent to acquaint their ^{1}H NMR spectra of COEs.

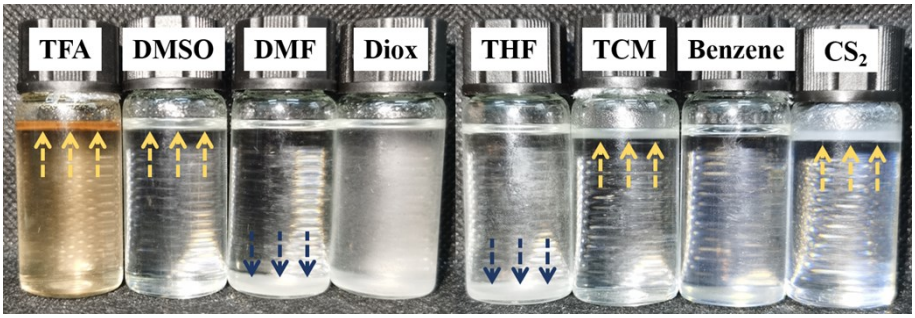

Fig. S3 Digital images of COE suspension after standing for 48 h. S400-T4 (20 mg) was dispersed in trifluoroacetic acid (TFA), dimethyl sulfoxide (DMSO), N, N-dimethylformamide (DMF), 1,4-

dioxane (Diox), tetrahydrofuran (THF), trichloromethane (TCM), benzene, and carbon disulfide (CS_2), respectively.

8. Digital images of the synthesized COEs

A series of COEs were obtained by mechanochemical esterification of regenerated cellulose and oleic acid via ball milling, and the state of different COEs was controlled by the reaction conditions. As seen in Fig. S4, the obtained S300-T4, S300-T6, and S400-T2 were grey powder because the rotational speed was too low or the reaction time was too short to meet the satisfactory mechanochemical esterification. When the mechanical force was intensified, the obtained COEs tended to aggregate to monolithic bulk due to the intrinsic plasticity.

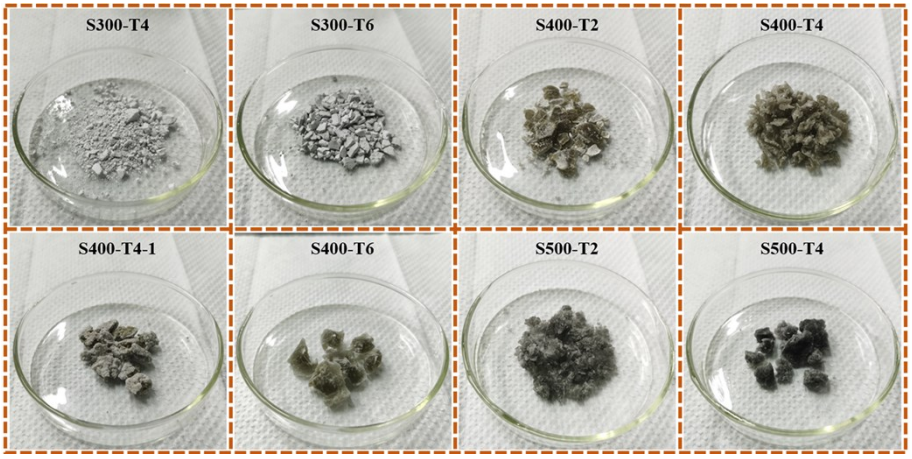

Fig. S4 Digital images of COEs synthesized under different conditions.

9. Characterization of MCC and RCC by POM

A small piece of the MCC (or RCC) was sandwiched between two cover glasses and observed on a POM. Numerous banded and fibrous birefringent domains were found clearly in the POM image (Fig. S4c) of MCC powder representing cellulose I crystals. In contrast, no obvious birefringent domain was observed in Fig. S4d, indicating the amorphous structure of RCC.

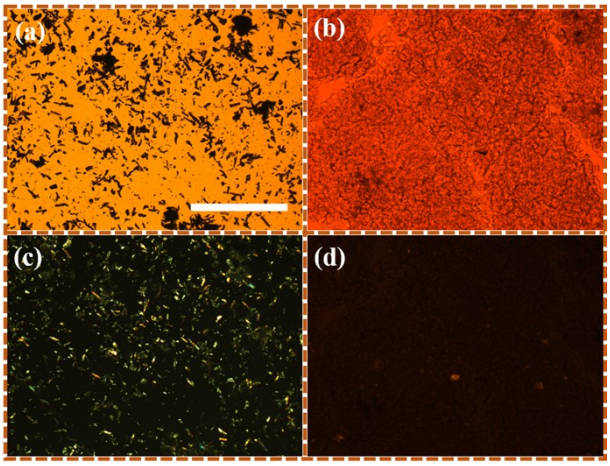

Fig. S5 (a, b) OM images of MCC and RCC, separately; (c, d) corresponding POM images. The bar of (a) represented 500 μm.

10. Crystalline structures of RCA and COEs

As shown in Fig. S5, conspicuous diffraction peaks at 12.1°, 20.5°, and 22.0° were observed in the WAXD curve of RCA, which were corresponded to the (1-10), (110), and (020) crystal planes of cellulose II crystals[8, 9]. The crystalline structures of COEs were changed when oleic side chains were chemically attached to cellulose backbones by the mechanochemical esterification, and only a broad peak was recorded at 19.8° represented the amorphous structure.

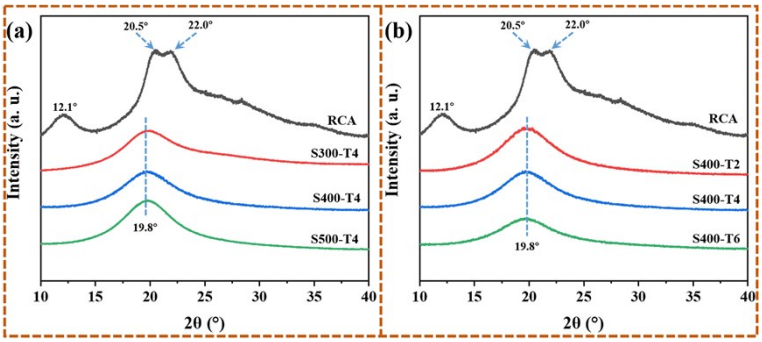

Fig. S6 WAXD spectra of RCA and COEs obtained under various conditions. (a) Different rotational speeds; (b) different reaction times.

11. DSC measurements of the prepared COEs

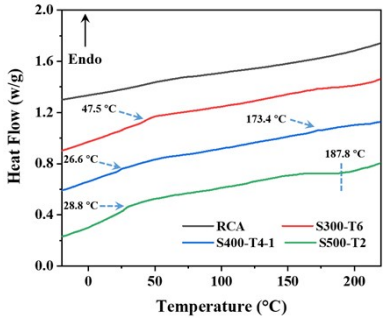

Fig. S7 DSC thermograms of RCA, S300-T6, S400-T4-1, and S500-T2.

12. Rheological temperature ramp test of the prepared COEs

To better understand the thermoplasticity of the obtained COEs, the hot-pressing COEs sheet (Φ 25 mm * 400 μm) were prepared for the temperature ramp test of the rheological behavior, and the measurement was carried out on a stress-controlled rheometer (TA Instruments, AR 2000ex) from 30 to 230 °C in a nitrogen atmosphere. During the test, the applied strain and frequency were 0.1% and 1 Hz, respectively, and the normal stress was fixed at 10 N. As seen in Fig. S8, the obtained thermoplastic COEs can be softened at 130 ~ 152 °C in the heating process depended on the DS values confirmed by the decreased storage modulus (G'), loss modulus (G''), and complex viscosity(|η*|), which indicated the thermoplastic transition of the products. Moreover, the "transition temperature" of the COE was decreased roughly as the content of oleoyl groups increased due to the internal plasticization of side chains except for S500-T4. Here, we did not analyze the detailed G', G'', and |η*| values of every sample due to inevitably excessive volume expansion of the products during the temperature ramp test of the rheological behavior (Fig. S9), additionally, the extrusive melt also had side effects on the G', G'', and |η*| values.

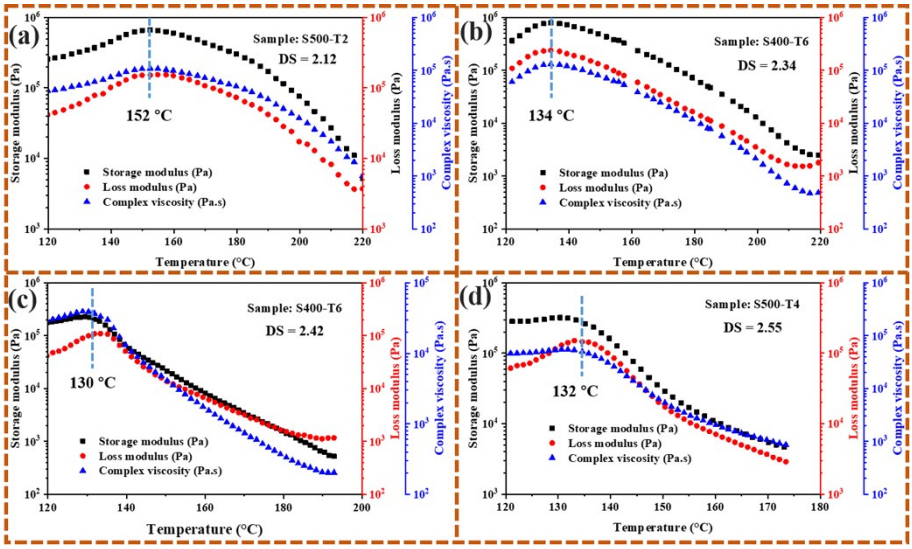

Fig. S8 Rheological behavior of the thermoplastic COEs (S500-T2, S400-T4, S400-T6, and S500-T4) under temperature ramp test.

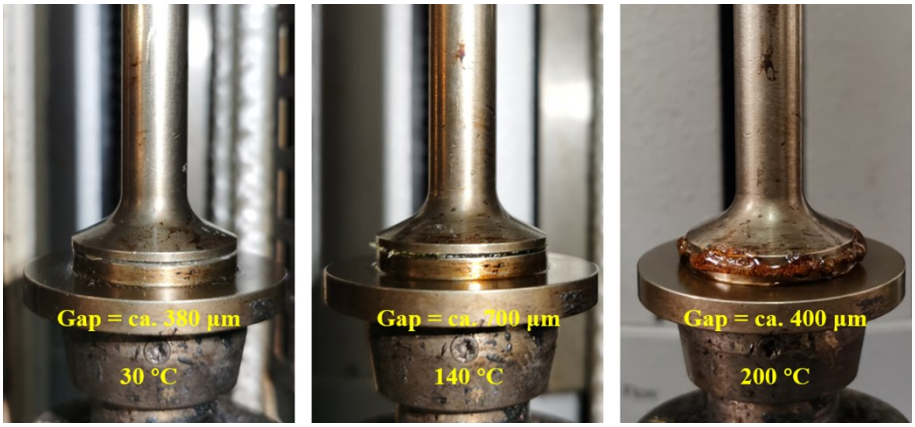

Fig. S9 Digital images of the S400-T4 sheet sandwiched between two coppery plates of rheometer during the temperature ramp test of the rheological behavior.

13. Thermostability of the prepared COEs

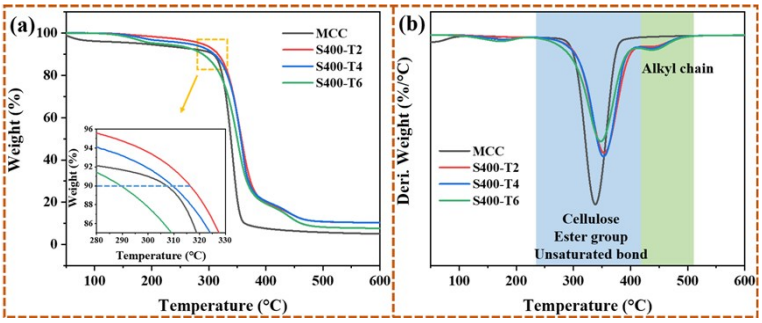

Fig. S10 TGA (a) and DTG (b) curves of MCC and COEs prepared under different reaction times when the rotational speed was fixed at 400 rpm.

Table S1 Thermal properties of the prepared COEs.

Samples	DS	T_g/°C[a]		T_d/°C[b]	T_{max}/°C[c]	
MCC	N/A[d]	N/A	N/A	307	338	N/A
S300-T4	1.29	57.3	N/A	342	371	442
S300-T6	1.63	47.5	N/A	330	363	445
S400-T2	1.79	28.2	172.5	316	354	438
S400-T4	2.34	25.8	164.7	309	353	439
S400-T4-1	1.74	26.6	173.4	292	362	442
S400-T6	2.42	27.6	153.8	289	348	443
S500-T2	2.12	28.8	N/A	320	363	440
S500-T4	2.55	25.6	N/A	301	354	440

a. T_g values were obtained from the DSC measurements; *b*. T_d represented the temperature of 10% weight loss in the TGA curve; *c*. T_{max} represented the temperature at the maximum weight loss peak in the DTG curve; *d*. The designated items were not available.

14. Morphology of the hot-pressing COE films

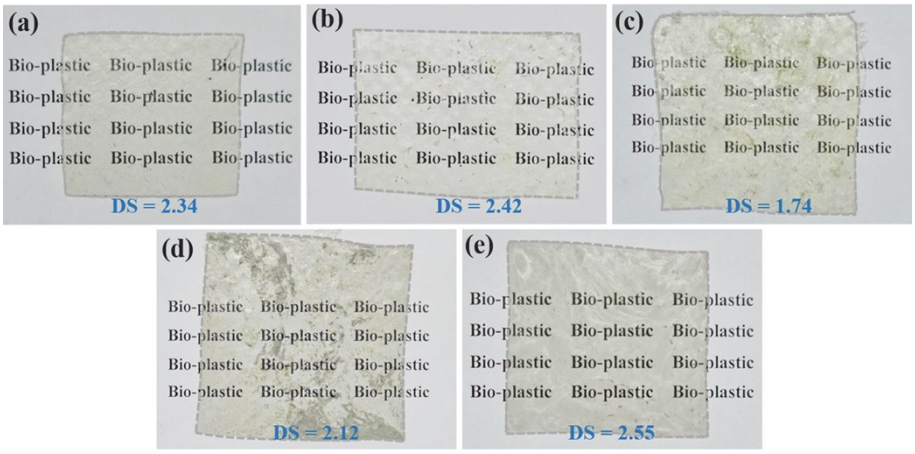

Fig. S11 Digital images of COE films. (a) S400-T4; (b) S400-T6; (c) S400-T4-1; (d) S500-T2; (e) S500-T4.

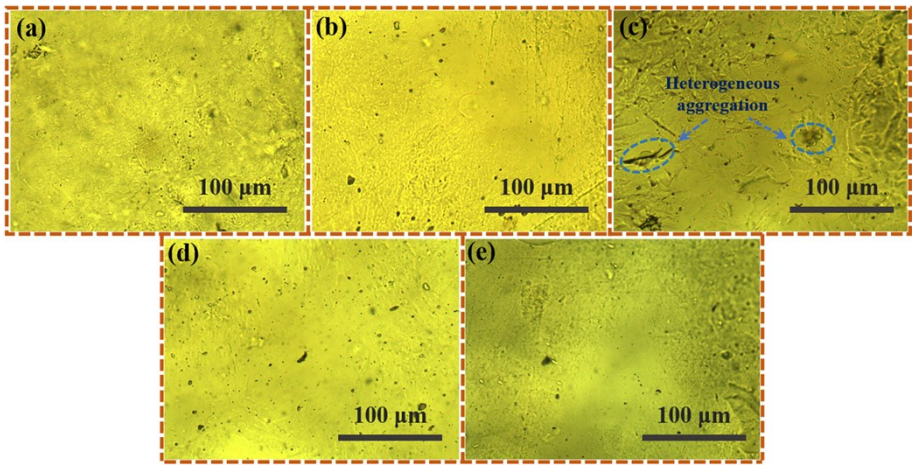

Fig. S12 Optical microscope (OM) images of the surface of COE films. (a) S400-T4; (b) S400-T6;

(c) S400-T4-1; (d) S500-T2; (e) S500-T4.

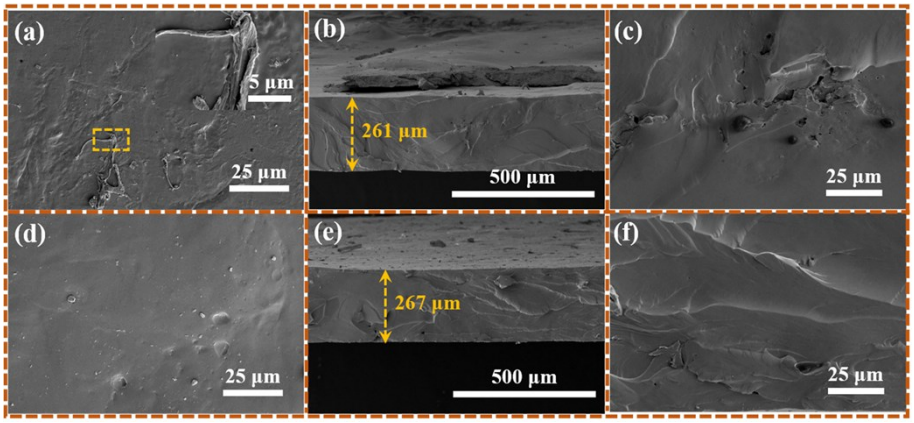

Fig. S13 SEM images of S400-T4-1(a-c) and S500-T2 (d-f) films, respectively. (a, d) surface morphology; (b, e) cross-sectional morphology; (c, f) magnified cross-sectional morphology.

References

1. D.-F. Hou, Z.-Y. Liu, L. Zhou, H. Tan, W. Yang and M.-B. Yang, *Int. J. Biol. Macromol.*, 2020, **161**, 177-186.
2. D.-F. Hou, H. Tan, M.-L. Li, Y. Tang, Z.-Y. Liu, W. Yang and M.-B. Yang, *Cellulose*, 2020, **27**, 8667-8679.
3. A. Isogai and R. H. Atalla, *Cellulose*, 1998, **5**, 309-319.
4. G. Samaranayake and W. G. Glasser, *Carbohydr. Polym.*, 1993, **22**, 1-7.
5. K. J. Edgar, T. J. Pecorini and W. G. Glasser, in *Cellulose Derivatives*, American Chemical Society, 1998, vol. 688, ch. 3, pp. 38-60.
6. Z. Huang, Y. Tan, Y. Zhang, X. Liu, H. Hu, Y. Qin and H. Huang, *Bioresour. Technol.*, 2012, **118**, 624-627.
7. R. K. Singh, P. Gupta, O. P. Sharma and S. S. Ray, *J. Ind. Eng. Chem.*, 2015, **24**, 14-19.
8. A. D. French, *Cellulose*, 2014, **21**, 885-896.
9. J. A. Sirviö, *Journal of Materials Chemistry A*, 2019, **7**, 755-763.